RSC Advances

This article can be cited before page numbers have been issued, to do this please use: A. Krishnan, T. S. Sreeremya, P. M. A, H. U. N. Saraswathy and S. Ghosh, *RSC Adv.*, 2015, DOI: 10.1039/C4RA17326K.

ROYAL SOCIETY OF CHEMISTRY

www.rsc.org/advances

View Article Online
DOI: 10.1039/C4RA17326K

Graphical abstract

Concentration quenching in cerium oxide dispersions via a Förster resonance energy transfer mechanism facilitates the identification of fatty acids.

Asha Krishnan, Thadathil S. Sreeremya, Unnikrishnan Saraswathy Hareesh and Swapankumar Ghosh*

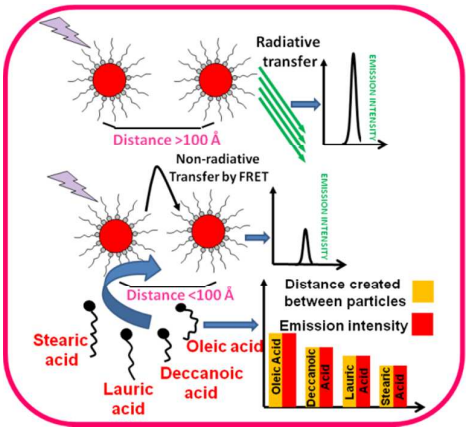

The distance dependence of FRET has been utilized, as a simple and novel analytical tool, for explaining the fluorescence quenching of cerium dioxide dispersions and in the prediction of structure of fatty acids.

View Article Online
DOI: 10.1039/C4RA17326K

Journal Name

Cite this: DOI: 10.1039/c0xx00000x

www.rsc.org/xxxxxx

ARTICLE TYPE

Concentration quenching in cerium oxide dispersions via a Förster resonance energy transfer mechanism facilitates the identification of fatty acids.

Asha Krishnan,[a] Thadathil S. Sreeremya,[a] A. Peer Mohamed,[a] Unnikrishnan Saraswathy Hareesh[a] and Swapankumar Ghosh*[ab]

Received (in XXX, XXX) Xth XXXXXXXXX 20XX, Accepted Xth XXXXXXXXX 20XX
DOI: 10.1039/b000000x

The energy exchange phenomena of cerium oxide based nanoparticles in a medium have been inspected by means of a meticulous approach. A concentration dependent non-radiative pathway has been revealed to the particles due to the close proximity between them which rendered the extinction of fluorescence. The calibration plot according to the Stern-Volmer equation showed a good linear relationship within the error limit and the value of Q denoting exchange interaction was close to 6 implying dipolar coupling between particles. Theoretical analysis of spectroscopic data exposed that Forster resonance energy transfer (FRET) is the dominant mechanism responsible for the interparticle excitation transfer and the Forster radius (R_0) calculated was 68.6 Aº. The distance dependence of FRET has been utilized to explicate the conformation and chain length of fatty acids by interrupting the energy transfer efficiency between particles and thus a simple analytical tool based on FRET for the qualitative as well as quantitative assessment of fatty acids have been projected.

Dynamic Article Links ►
View Article Online
DOI: 10.1039/C4RA17326K

Cite this: DOI: 10.1039/c0xx00000x

www.rsc.org/xxxxxx

ARTICLE TYPE

Introduction

The physical dimensions of semiconductor nanocrystals often serve as a resource of innovative photochemical properties owing to quantum confinement when their dimension is less than their corresponding Bohr exciton radius as well as Debye length which usually falls in the nanometer range. These 'artificial atoms' are called as quantum dots and their zero dimension restricts the number of electrons which imparts the quantization of energy levels in the density of states (DOS).[1] The most fascinating outcome of this phenomenona is the widening of band gap and its resultant blue shift. The influence of nano dimension on the band gap endorses the tunability of the optical properties of nanoparticles and therefore a wide range of application is renderd by the size dependent properties.[2]

Cerium dioxide is a distinguished semiconductor and is extremely useful for its luminescence, non toxicity, high refractive index, chemical and thermal stability etc.[3-7] On account of its properties, cerium oxide have been employed as an oxygen reservoir, catalyst, gas sensor, abrasive etc.[8] In fact while the Bohr radius and Deye length of ceria has been taken into account which is ~7 nm and 3 nm respectively the ceria based nano structures with appropriate dimensions are proficient in exhibiting innovative optical properties.[9,10] Few reserach groups have reported a blue colored emission of ceria nanoparticles when their aspect ratio shrinked below 3 nm.[6] With reference to the studies by Tanigucchi *et al.*, a luminescence quantum yield of 59% was achieved by ceria comprising a sheet like morphology.[11] In the light of the scarcity of superlative luminescent materials, the control and improvement of the properties of existing nano phosphors have always been a major aspiration in the world of research.[12] In the aspect of designing efficient phosphor materials, phenomena like luminescence enhancement, quenching, delay in emission, decay rate etc. deserves vital significance. Among these, quenching of luminescence is a prevailing phenomenon which is highly undesirable due to the resulting reduction in overall quantum yield, which in turn affect the luminescence efficiency. But it is a bit astonishing reality that even the adverse phenomenon needs be probed for many functional applications like molecular sensing, imaging, drug release profiling, DNA detection etc. if the underlying quenching mechanism is thoroughly understood.[13,14]

Different pathways has been proposed so far for clearing up the mystery behind fluorescence quenching, from simple collisional energy exchange to nanoparticle surface energy exchange (NSET).[15,16]In the present study, various spectroscopic tools has been employed to investigate the existence of a non-radiative energy transfer mechanism between ceria nanoparticles based on the principle of Forster Resonance Energy transfer (FRET). FRET is a distant energy transfer process making use of dipolar pairing between donor and acceptor molecules.[17] Due to its dependence on distance, FRET has now emerged as convenient technology at the single molecular detection limit and is found suitable for studying the distance between two molecules or two neighboring sites on a specific macromolecule, during protein conformational change, protein interaction, enzyme activity.[18-24]Since FRET physically originates from the weak electromagnetic coupling of two dipoles, introducing additional dipole like metal nanoparticles provides more coupling interactions and thus FRET efficiency can be.[25] There have been many recent efforts for the development of fluorescence assays based on this principle for applications like DNA detection. Mirkin *et al.* developed a method for the analysis of DNA which is based on gold nanoparticles.[26]

Also there are studies involving quantum dots as FRET pairs on account of its high photo stability, great emission intensity and photo bleaching resistance. Their broad absorption and narrow emission spectra allow single-wavelength excitation of multiple donors and can avoid crosstalk with acceptor fluorophores. They can also be coupled to multiple acceptor fluorophores for higher efficiency in energy transfer and can act as the support structure for biomolecules for imaging purposes or to simplify assay design.[14] Leong *et al.* has developed a single-step quantum dot-mediated FRET system to investigate the structural composition and *in vitro* dynamic behaviour of plasmid DNA hybrid nanostructure.[27] Song *et al.* designed a positively-charged, compact QD–DNA complex for the detection of nucleic acids.[28]

Here in we have incorporated the principle of FRET with quantum dots based on ceria which served as a facile analytic model for the identification of fatty acids. Monodisperse ceria nanoparticles of average size ~2 nm were synthesised by adopting a thermal decomposition strategy. The size induced optical properties e.g., fluorescence exhibited by the ceria crystals while approaching nano size have already been reported earlier.[29] In the present study, attempt has been made to evaluate the mechanism behind the concentration dependent quenching of the fluorescence. Despite the significant research activity in field of nano cerium dioxide in recent years, this manuscript is the first to report a FRET based energy transfer mechanism in cerium dioxide nano system. Also efforts have been made to mould the quenching mechanism as an effective tool for the identification of fatty acids.

Experimental Section

Materials and Synthesis

All the chemicals were used as received without further purification. Cerium acetate (99.9%), stearic acid (90%) and lauric acid (90%) were purchased from Merck, India. Diphenyl ether (99%), deccanoic acid (90%) and oleyl amine (70%) were procured from Sigma Aldrich and oleic acid (90%) from Alfa Aesar, UK. Commercial olive oil (extra virgin olive oil) has been procured from Jindal Retail (India) Pvt. Ltd. Common solvents

View Article Online
DOI: 10.1039/C4RA17326K

such as acetone, ethyl alcohol, cyclohexane and toluene (analytical grade) were procured from Merck, India.

The precursor employed in the present synthetic strategy was cerium acetate which is decomposed upon supply of heat in diphenyl ether solvent to form ceria. In a typical synthesis, 0.005 moles of cerium acetate was dissolved in 100 ml diphenyl ether in a round bottom flask. Oleic acid was utilized to functionalize the surface of synthesized nanoparticles. About 0.02 mole oleic acid and 0.023 mole oleylamine were added to the reaction mixture and were refluxed at its natural boiling point (~260 °C) for 1 h. Oleic acid, in the presence of oleyl amine is expected to undergo ionization to form the corresponding oleate ion which is capable of coordinating with the positive core of the nanoparticles formed. As the reaction proceeded, the solution turned brown, indicating the formation of ceria nanocrystals. After the reaction time, the mixture was allowed to cool to room temperature. Subsequently, acetone was added to the reaction mixture to precipitate the oleic acid coated nanoparticles. The precipitate obtained was separated by centrifugation and washed thoroughly with acetone several times to get rid of excess oleic acid. Finally, after washing, the precipitate was dried in an air oven to slightly brownish powder. The particles could easily be dispersed in nonpolar solvents e.g., hexane, toluene etc. indicating the successful surface modification by oleic acid.

A parent dispersion of ceria nanoparticles in toluene has been prepared by suspending 0.01 g dried nanoparticles in 25 ml toluene (0.002 M) and sonicated for about 10 min. Ceria dispersions of different concentration have been prepared from this parent suspension upon dilution. Dispersions having concentrations in the range 0.0001-0.0018 M have been prepared by dilution followed by sonication for 10 min. For the estimation of oleic acid in real sample, 2 ml of commercial olive oil was added to a 0.00018M ceria dispersion and photoluminescence spectrum was collected.

Instrumental techniques

The X-ray diffraction (XRD) patterns of the dried and powdered specimens were obtained using a Philips X'PERT PRO diffractometer with Ni-filtered Cu Kα1 radiation (λ = 1.5406 Å) using 30 mA current at 40 kV. Powder samples were scanned in the continuous scan angle range 5-100 degree (2θ) at a scanning speed of 2 degree per min with a step size 0.04°. The morphology and average size of the nanocrystals were investigated by high resolution transmission electron microscopy (HR-TEM) using a FEI Tecnai 30 G2 S–Twin microscope operated at 300 kV and equipped with a Gatan CCD camera. A small amount of the nanoparticles were dispersed in toluene and ultrasonicated to get a stable suspension. Samples for TEM study were prepared by dropping a microdroplet of the suspension on to a 400 mesh copper grid and drying the excess solvent naturally. Size measurements for the cerium oxide in suspension were carried out at 25 °C by photon correlation spectroscopy (PCS) on a Zetasizer 3000 HSA, Malvern Instruments, Worcestershire, UK using a 60 mW He–Ne laser producing 633 nm wavelength with General Purpose algorithm with Dispersion Technology Software (v. 1.61) at 90° detection angle. Fourier transform infrared (FTIR) spectra of the as prepared products were recorded at room temperature using KBr (Sigma Aldrich, 99%) pellet method on a Nicolet Magna IR-560 spectrometer in the 400 to 4000 cm^{-1} range. The absorption spectra of the samples were obtained using a UV–visible 2401 PC spectrophotometer (Shimadzu, Japan) in the wavelength range 200–800 nm. The PL spectrum of the surfactant coated nanoparticle suspension in toluene was taken at room temperature using a Cary Eclipse spectrofluorometer (Varian, Australia). Fluorescence lifetimes were measured using IBH (FluoroCube) time-correlated picoseconds single photon counting (TCSPC) system. Nanoparticles dispersions were excited with a pulsed diode laser (<100 ps pulse duration) at a wavelength of 400 nm (NanoLED-11) with a repetition rate of 1 MHz. The detection system consisted of a microchannel plate photomultiplier (5000U-09B, Hamamatsu) with a 38.6 ps response time coupled to a monochromator (5000 M) and TCSPC electronics (Data station Hub including Hub-NL, NanoLED controller and preinstalled Fluorescence Measurement and Analysis Studio (FMAS) Software).

Results and discussion

Preliminary characterization

The synthetic approach employed for the present study is based on a one-step thermal decomposition of cerium acetate in diphenyl ether reported earlier.[29] The mechanism behind the nucleation of nanoparticles by this approach which involves the formation of free radical intermediates is also a well established phenomenon.[30]According to the published literature, oleic acid in presence of oleyl amine undergoes dissociation to form oleate ions and its negatively charged carboxylate head chemisorbs on to the positively charged nanoparticle core. In the FT-IR spectrum (please see Fig. S5 in ESI), two peaks at 1433 and 1515 cm^{-1} due to the stretching vibration of carboxylate group confirm the presence of oleate group chemisorbed on the nanoparticle surface.[31] Therefore, the nanoparticles formed will comprise of a monolayer of surfactant on the particle surface. The X-ray diffractograms of the particles synthesized in this report and its TEM images are shown in Fig. 1 (please see S1 in ESI also). The XRD patterns fitted well with the cubic fluorite phase of ceria (according to JCPDS card no. 34-0394) and the nanocrystalline nature of the particles was evidenced by the broadening of the peaks.[32,33] An anomalous small peak observed at a 2θ value of approximately 20º is attributed to the presence of oleic acid surfactant.[34] The TEM images confirms the formation of ultra fine and fairly uniform sized ceria nano crystals with spherical morphology. The high resolution images indicate that the nanoparticles are single crystals and selected area diffraction (SAED) pattern shows (111), (200), (220), and (311) Debye-Scherrer rings with corresponding interplanar spacings of 0.31, 0.27, 0.19, and 0.16 nm (Fig. S2).

View Article Online
DOI: 10.1039/C4RA17326K

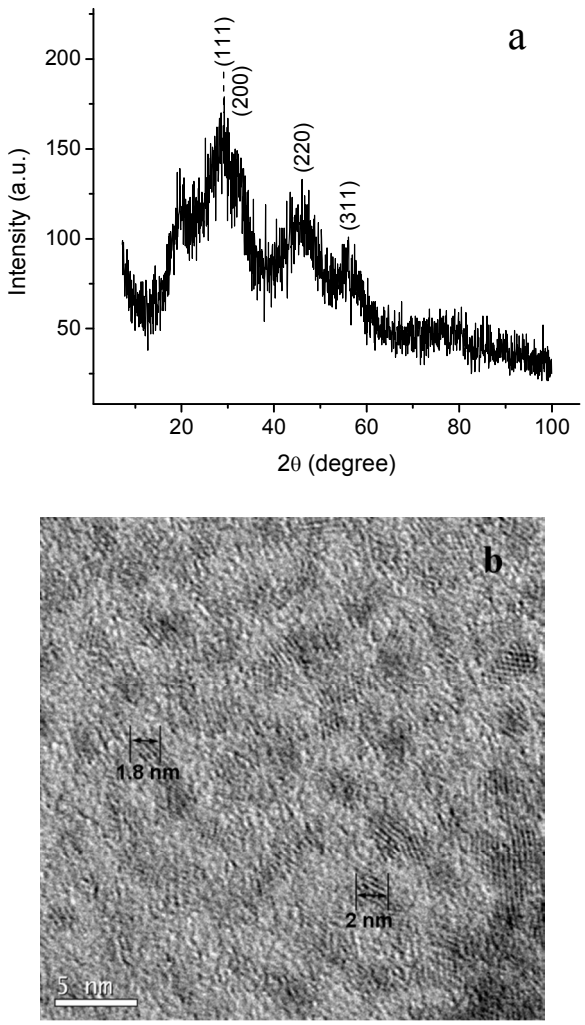

Fig. 1 (a) XRD patterns and (b) HR-TEM image of the as synthesized ceria nanoparticles.

The average particle size derived from multiple TEM images was 2±0.17 nm. After surface modification, the alkyl tail of the fatty acid protrudes out of the nanoparticle surface. The sterric repulsion imparted by the fatty acid chain prevents the nanoparticles to come closer and the particles will remain well dispersed as evidenced by TEM. The particles were dispersible in non-polar solvents owing to the hydrophobic surface endowed by the oleic acid surfactant. The photon correlation spectroscopy data for the nanoparticles in toluene dispersion (Fig. S3 of electronic supplementery information) gives the hydrodynamic size as 3.9 nm which matches well with the TEM obervation when the chain length of the surfactant being considered.[35,36]

Optical properties and fluorescence quenching

The absorbance and emission spectra, photoluminescence measurements at different concentrations and its dependence on concentration of the nanoparticles dispersions in toluene is shown in Fig. 2. One of the notable features of the absorbance spectra is its broadness over almost the whole visible region. The emission spectra (λ_{ex} = 400 nm) was also fairly broad with an emission maximum at about 510 nm. The broadness in the optical spectra has been attributed to the creation of defects in the system during the process of nanoscaling of the crystals.[29]

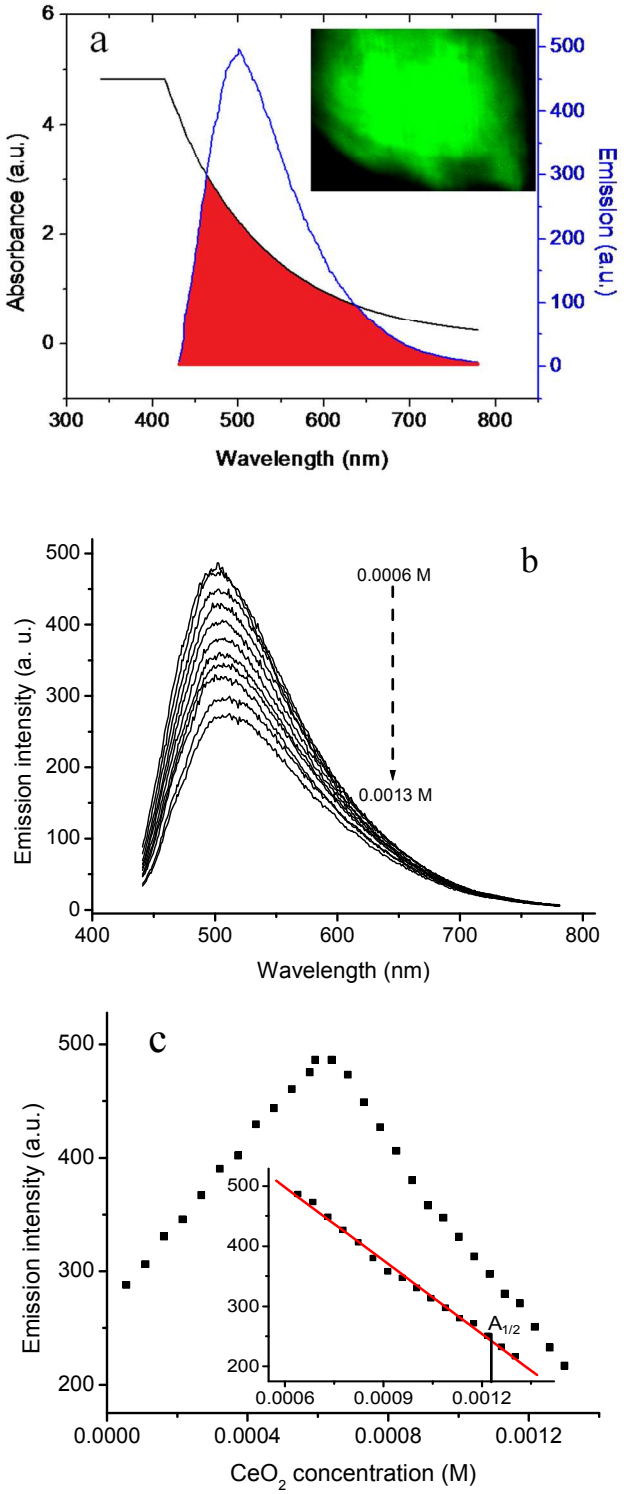

Fig. 2 (a) Absorption and emission spectra of the nanoparticles, the shaded portion showing the spectral overlap, the inset showing green coloured emission, (b) emission spectra of the dispersion at different concentrations (0.0001-0.0013 M) and (c) variation of emission intensity with concentration. The inset shows the linearly fitted portion of the quenching region alone.

View Article Online
DOI: 10.1039/C4RA17326K

The emission in the green region showed an initial rise in intensity with concentration and after reaching a maximum, emission intensity seemed to decrease linearly. The inset of Fig 2c shows the linearly fitted portion of the graph which shows quenching. Fluorescence quenching is generally described by the Stern–Volmer eqn (1)

$$\frac{I_0}{I} = 1 + K_{SV}[Q] \qquad (1)$$

where I_0 and I are the fluorescence intensity of fluorophore in the absence and presence of quencher respectively, [Q] indicates the concentration of quencher and K_{SV} is Stern-Volmer quenching constant.[37] As there is no external quencher in the present system, the Stern-Volmer equation has been modified and plotted I_0/I against [Q] as shown as Fig 3a. Here I_0 is the emission intensity of the parent dispersion whose concentration does not fall in the quenching range (0.000639 M) and [Q] is the concentration of the dispersion added to a fixed volume of parent suspension. The variation in intensity against solid concentration is almost linear as indicated by near perfect linear regression with a R^2 value of 0.9902 which indicates effective quenching.

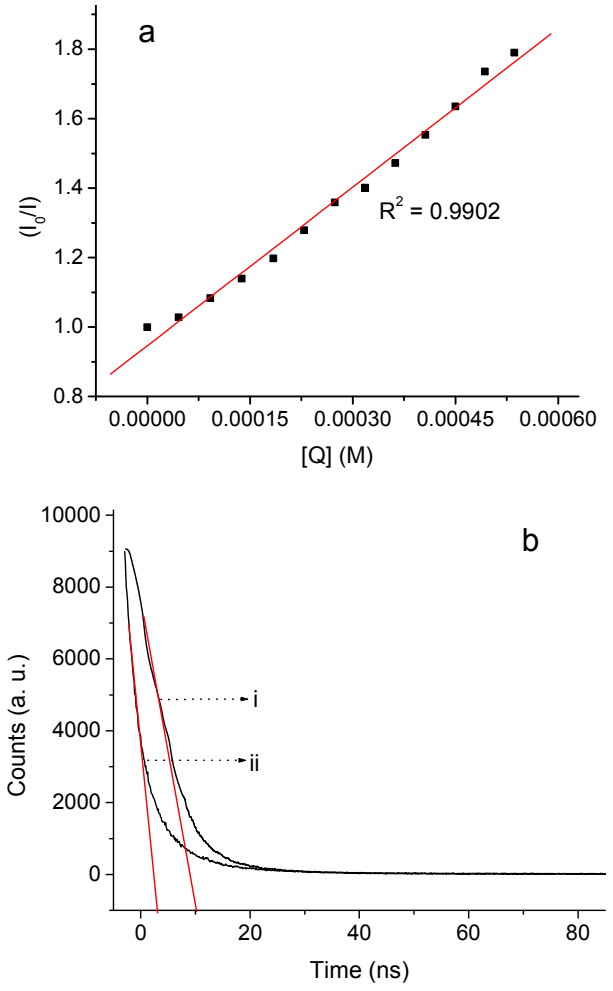

Fig. 3 (a) Stern-Volmer plot for the concentration quenching of the dispersions and (b) fluorescence life time measured for the dispersion at concentrations (i) 0.000868 M and (ii)0.0013 M.

The life time of the excited state measured for dispersion at two different concentrations (0.000868 and 0.0013 M) yielded different values, 10 and 3 ns respectively as depicted by Fig. 3b. The emission intensity can be related to lifetime according to the equation $I = A\ e^{-(E/kt)}$, where A is a constant, k is the decay constant and t is the life time.[38] It is accounted that the closeness of the nanoparticles with increasing concentration paved way to a faster energy relaxation mechanism without radiative emission. The particles could transfer the excess energy within 3 ns in a non-radiative pathway which resulted in the quenching of fluorescence.

Quenching mechanism based on FRET

Many mechanisms like complex formation, collisional processes and other energy transfer methods has been proposed so far for the quenching effects.[15,39] As in the present system, the nanoparticles are sterically well spaced by bulky oleic acid groups, the former two mechanisms can be ruled out. Moreover the fast fluorescence decays for concentrated dispersions within the first 3 ns is a clear signature of non-radiative energy transfer.[40] The absorbance and emission spectra of the nanoparticles shows considerable spectral overlap indicated by the shaded region in Fig. 2a which index towards a Forster resonance energy transfer (FRET) mechanism for the quenching effects. Förster resonance energy transfer (FRET) is a distance dependent energy transfer process in which energy is transferred from an excited donor to an acceptor molecule through a dipole-dipole interaction. An efficient FRET demands certain conditions to be satisfied like (i) the spectral overlap of donor emission and acceptor absorbance spectra, (ii) a desirable distance between the donor and acceptor and (iii) possibility of dipole-dipole interaction.[13,14,17,41,42]

The significance of spectral overlap lies in the fact that a ground state acceptor could be energetically transferred to a higher level on the expense of an excited donor. Fig. 2 depicts that there is a considerable spectral overlap between absorption and emission of nanoparticles from about 450 to 750 nm (layer a). The absorption shoulder (λ_{max}) is at 400 nm and the maximum emission peak is at ~510 nm. Both the spectra were fairly broad which extends over almost the whole visible range. It is noteworthy that the effective overlap of the spectra has been brought into reality by this extensive spreadness over the whole wavelength under consideration. As the spectral broadening had originated from the defects associated with the miniaturization of the crystals, the root of quenching effect lies on the the nano dimension of the system.[29,43] So in the present system, the optical spectra of the nanoparticles are in favour of the energy transfer between themselves through a FRET mechanism.

As pointed out earlier, the energy transfer by FRET is accomplished through a dipole–dipole interaction between the transition dipole moments of the acceptor and donor.[17] Therefore the detailed investigation of the interaction between nanoparticles during emission cannot be evicted. The alignment of dipole moment is a prevailed phenomenon in cerium dioxide owing to the electronegativity of oxygen. Therefore, the interaction of crystals on account of the dipole moment is highly probable in ceria. In fact, there are many reports which supports the existence

View Article Online
DOI: 10.1039/C4RA17326K

of dipole–dipole interaction in ceria during the coarse of investigation of crystal growth and morphology evolution.[44,45]

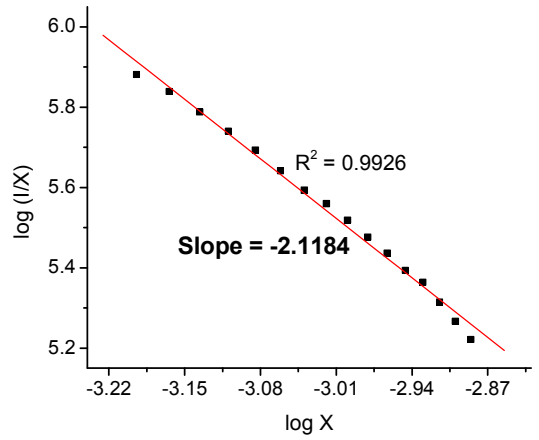

Fig. 4 Plot of log(I/X) against log X fitted linearly to show dipole-dipole interaction between particles.

According to Dexter's theory on energy transfer, the source of interaction which resulted in concentration quenching can be estimated using the eqn (2)

$$\frac{I}{X} = \frac{K}{[1+\beta(X)^{Q/3}]} \qquad (2)$$

in which I/X is the emission intensity per quencher concentration, Q is the exchange interaction whereas K and β are constants for a given lattice.[46] The value of Q is the significant factor which reveals the type of interaction. Q = 6, 8 or 10 for electric dipole–dipole (D–D), electric dipole–quadrupole (D–Q), or electric quadrupole–quadrupole (Q–Q) interactions respectively.[12,38,46] The slope of the linear fit of the log (I/X) versus log X data gives the value of Q. The Q value calculated for the present system from Fig. 4 is 6.36 (slope = -2.12, Q = -3*slope) which is closer to 6 indicating a dipole-dipole interaction.

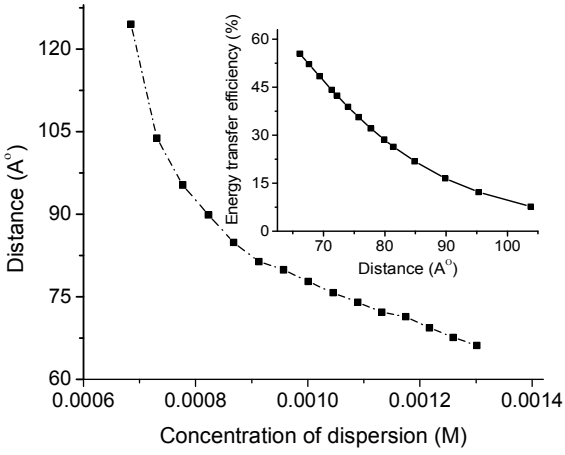

Fig. 5 Variation of distance between particles with concentration of dispersion. The inset shows enhancement in energy transfer efficiency with decrease in interparticle distance.

The prerequisite of close proximity in FRET limits the distance between donor and acceptor in the order of 100 Å owing to the dipole-dipole interaction. For distance estimation, we considered the Förster radius (R_0) which is the critical distance between the donor and acceptor at which the energy transfer rate is 50%.[42] R_0 can be calculated according to the eqn (3)

$$R_0 = \frac{7.35}{\left([A]_{1/2}\right)^{1/3}} \qquad (3)$$

where $[A]_{1/2}$ is the half-quenching concentration, the concentration at which emission intensity is reduced to half.[47] According to Forster theory, the energy transfer rate at different distances can be calculated as

$$E = 1 - \frac{I}{I_0} \qquad (4)$$

using which the energy transfer rates of the dispersions at the concentrations under study can be estimated.[48] But there is also another equation relating R_0 and E which is given as

$$E = \frac{R_0^6}{(R_0^6 + r^6)} \qquad (5)$$

where 'r' refers to the distance between the particles corresponding to the energy transfer rate.[48] Therefore, it is possible to estimate the distance between particles at concentrations which is falling in the quenching region by knowing the corresponding value of emission intensity.

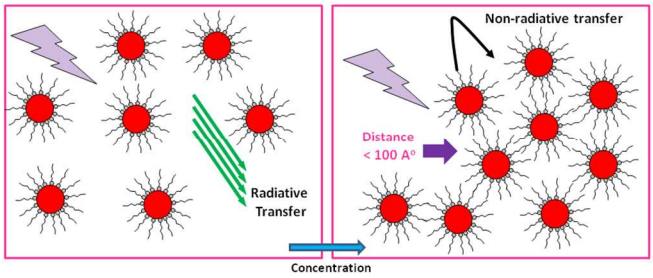

Scheme 1 Mechanism proposed based on FRET for the concentration quenching of ceria dispersions.

The $[A]_{1/2}$ calculated from the linear regression (inset of Fig 2c) was 0.001229 M and the value obtained for R_0 using equation (3) was 68.6 Å. The r value calculated at different concentrations using eqn (3), (4) and (5) was plotted against its corresponding concentration and is shown graphically in Fig. 5. It was observed that the distance calculated between particles for concentrations in the quenching range falls in the order of 100 Å which is supporting the proposed mechanism. The inset of Fig. 5 shows the enhancement in energy transfer efficiency when the separation between particles is deteriorating. As the particles are approaching closer, the dipoles are freed to interact more effectively which amplified the energy transfer rate. The quenching phenomenon was not observed for dilute dispersions likely due to the absence of a proximal acceptor particle within the desired distance range of FRET. Scheme 1 represents the summary of the mechanism.

Effect of spacers on quenching

As FRET is a quenching mechanism highly sensitive to distance between the flurophores, the presence of any moiety in the dispersion, capable of changing the distance between the particles

View Article Online
DOI: 10.1039/C4RA17326K

can cause a divergence in quenching rate. The impact can be visualised in the emission spectra of the corresponding dispersion and it can perform as the source of structural identification of the moiety. In the present study, such a moiety which may come in between the particles other than solvent is denoted as a 'spacer'. Fatty acids differing in chain length as well as structure such as deccanoic acid ($C_{10}H_{20}O_2$), lauric acid ($C_{12}H_{24}O_2$), stearic acid ($C_{18}H_{36}O_2$) and oleic acid ($C_{18}H_{34}O_2$) have been used as spacers. To a fixed volume of concentrated dispersion (0.0018 M), a fixed volume (3.5 ml) of individual spacer was added and photoluminescence spectra were collected.

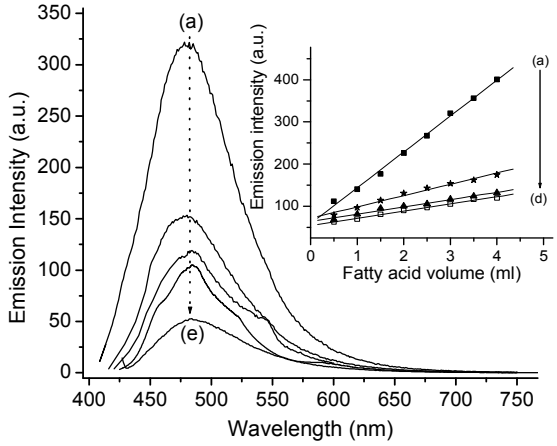

Fig. 6 Emission spectra of the dispersion after the addition of different spacers (a) oleic acid, (b) deccanoic acid, (c) lauric acid, (d) stearic acid and, (e) parent CeO_2 NP dispersion without addition of spacer. The inset shows the variation in emission intensity with increase in the concentration of spacers.

All the fatty acids accomplished an enhanced emission with respect to the parent dispersion and are shown in Fig. 6. The change in PL intensity of the CeO_2 dispersions as a function of different fatty acids and their volumes added are shown in the inset. Whereas oleic acid gave the maximum intense spectra, the emission intensity showed an inverse relation with chain length for the rest. Though the contribution of the spacer towards the overall dipole moment can enhance the energy transfer efficiency to a higher extent, it is least probable for the present system. This is because as electronic effects are not felt beyond three or four carbon, the difference in chain length alone is least expected to cause any marked influence on dipole moment.[49] Also the presence of double bond in the alkyl chain of oleic acid favours non-polar character in the chain which may in turn reduce dipolar nature in contrast to the observed result.[50] Therefore, an improvement in emission bestowed by the spacers is likely due to the separation induced by them in between the particles.

The manner in which surfactant like molecules align in a medium strongly depends on certain parameters like chain length compatibility, chain cohesion, molecular interactions etc. which contributes to the intermolecular distance.[49] As chain length increases, the van der Waals interaction between the chains of adjacent molecules increases and vice-versa.[49]

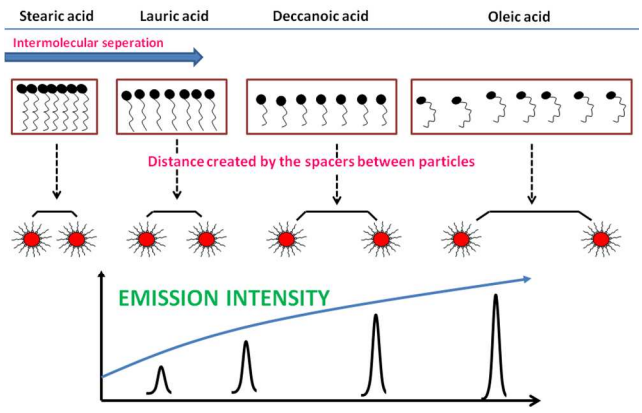

Scheme 2 Enhancement in emission intensity provided by the spacers by altering distance between particles.

In a medium, the extent of solvation solemnly depends on this attractive force, which in turn, affects the intermolecular separation.[51] For shorter fatty acids as attractive interaction is weak, molecules are farther to each other in the medium. For oleic acid, this intermolecular attraction is again weak due to the kink induced by the *cis*-bond at the C9 position.[51] Due to its inefficiency to remain closely packed as its straight chain colleagues, solvent could well separate these molecules. So the distance created by the spacers between the nanoparticles will be highly influenced by this intermolecular attraction which decides the order of enhancement provided by them in the emission as depicted in Scheme 2. Thus each spacer will leave its own signature in the emission spectra depending upon its structure and chain length. The linear increase in the emission intensity with the increase in the concentration of the spacers (inset fo Fig. 6) also substantaites the proposed rationale based on the structure of spacer.

The linear intensity versus concentration profiles shown as the inset of Fig. 6 allows the quantitative estimation of fatty acids as well. Atempt has been made to estimate the amount of oleic acid present in a commercially available olive oil. To a fixed volume of concentrated dispersion of CeO_2 (0.0018 M), 2 ml of commercial olive oil was added and photoluminescence spectra was collected. It was observed that the pholuminescence spectra of pure and commercial oleic acids showed little difference in PL intensity (Fig. S6) which gave a net oleic acid content in the commercial olive oil to ~85% (1.7 ml in 2 ml) which is close to the certified content of 86.5%. This data demonstrates the practical applicabilty of the proposed technique for the quantification of fatty acids.

Conclusions

A spectroscopic investigation of the concentration quenching behaviour of ceria nanoparticles in dispersion have been carried out. The particles exhibited a linear Stern-Volmer characteristic and the inter particle dipole interaction has been established by graphical interrogation. The distance calculated between particles according to Förster theory falls within the FRET limits which along with other theoretical explorations projected a mechanism based on Förster resonance for the transfer of electronic excitations. The hypersensitivity of FRET to distance ultimately

View Article Online
DOI: 10.1039/C4RA17326K

served as a yardstick to distinguish different fatty acids based on their structure and conformation. The present study supplies a model for the structural elucidation of molecules by means of a simple analytical approach.

Acknowledgments

The authors are thankful to Director, CSIR-NIIST for providing the necessary facilities for the work and CSIR-Central Glass & Ceramic Research Institute for continuing the same. Authors thank Department of Science & Technology and CSIR, India for providing HR-TEM facility to NIIST. Authors also acknowledge Mr. M. Kiran for the HR-TEM imaging and analysis. Authors gratefully acknowledge Mr. Nandajan and Mr. Akhil of NIIST for life time measurements. Authors AK and TSS acknowledge CSIR for the CSIR Fellowships. This work was partly funded by the Indian Rare Earths Limited Technology Development Council (IRELTDC), DAE, India.

Notes and references

[a] *Material Science and Technology Division, National Institute for Interdisciplinary Science & Technology (NIIST), Council of Scientific & Industrial Research (CSIR) Trivandrum-695019, India*

[b] *ACTC Div, Central Glass & Ceramic Research Institute, CSIR, 196 Raja S. C. Mullick Road, Kolkata-700 032, India. E-mail: swapankumar.ghosh2@mail.dcu.ie; ashakarthika7@yahoo.co.in Fax: +91-33-24730957; Tel: +91-33-23223546 Homepage: http://www.cgcri.res.in*

1 D. Bera, L. Qian, T.-K. Tseng and P. H. Holloway, *Materials*, 2010, **3**, 2260.

2 E. Jang, S. Jun, H. Jang, J. Llim, B. Kim and Y. Kim, *Adv. Mater.*, 2010, **22**, 3076.

3 T. J. Brunner, P. Wick, M. Manser, P. Spohn, R. N. Grass, L. K. Limbach, A. Bruinink and W. J. Stark, *Environ. Sci. Technol.*, 2006, **40**, 4374.

4 J. Zhang, S. Ohara, M. Umetsu, T. Naka, Y. Hatakeyama and T. Adschiri, *Adv. Mater.*, 2007, **19**, 203.

5 C. L. Chai, S. Y. Yang, Z. K. Liu, M. Y. Liao and N. F. Chen, *Chinese Sci. Bull.*, 2003, **48**, 1198.

6 S. Maensiri, C. Masingboon, P. Laokul, W. Jareonboon, V. Promarak, P. L. Anderson and S. Seraphin, *Cryst. Growth Des.*, 2007, **7**, 950.

7 H. Gu and M. D. Soucek, *Chem. Mater.*, 2007, **19**, 1103.

8 K. C. Remani and S. Ghosh, *Trans. Ind. Ceram. Soc.*, 2009, **68**, 185.

9 W. Shen, J. Jiang, C. Ni, Z. Voras, T. P. Beebe, Jr. and J. L. Hertz, *Solid State Ionics*, 2014, **255**, 13.

10 S. V. N. T. Kuchibhata, A. S. Karakoti, D. R. Baer, S. Samudrala, M. H. Engelhard, J. E. Amonette, S. Thevuthasan and S. Seal, *J. Phys. Chem. C*, 2012, **116**, 14108.

11 T. Taniguchi, Y. Sonoda, M. Echikawa, Y. Watanabe, K. Hatakeyama, S. Ida, M. Koinuma and Y. Matsumoto, *ACS Appl. Mater. Interfaces.*, 2012, **4**, 1010.

12 W. Z. Lv, Y. C. Jia, Q. Zhao, M. M. Jiao, B. Q. Shao, W. Lu and H. P. You, *RSC Adv.*, 2014, **4**, 7588..

13 P. C. Ray, G. K. Darbha, A. Ray, J. Walker and W. Hardy, *Plasmonics*, 2007, **2**, 173.

14 N.-T. Chen, S.-H. Cheng, C.-P. Liu, J. S. Souris, C.-T. Chen, C.-Y. Mou and L.-W. Lo, *Int. J. Mol. Sci.*, 2012, **13**, 16598.

15 M. Szabelski, D. Ilijev, P. Sarkar, R. Luchowski, Z. Gryczynski, P. Kapusta, R. Erdmann and I. Gryczynski, *Appl. Spectrosc.*, 2009, **63**, 363.

16 C. S. Yun, A. Javier, T. Jennings, M. Fisher, S. Hira, S. Peterson, B. Hopkins, N. O. Reich and G. F. Strouse, *J. Am. Chem. Soc*, 2005, **127**, 3115.

17 Y. H. Park, Y. Kim, H. Sohn and K. S. An, *J. Phys. Org. Chem.*, 2011, **25**, 207.

18 K. A. Krukenberg, T. O. Street, L. A. Lavery and D. A. Agard, *Q. Rev. Biophys.*, 2011, **44**, 229.

19 T. Krusinski, A. Ozyhar and P. Dobryszycki, *Nucleic. Acids Res.*, 2010, **38**, 11..

20 K. Boeneman, B. C. Mei, A. M. Dennis, G. Bao, J. R. Deschamps, H. Mattoussi and I. L. Medintz, *J. Am. Chem. Soc.*, 2009, **131**, 3828.

21 Y. Choi, J. Lee, K. Kim, H. Kim, P. Sommer and R. Song, *Chem. Commun.*, 2010, **46**, 9146.

22 Y. P. Kim, Y. H. Oh, E. Oh, S. Ko, M. K. Han and H. S. Kim, *Anal. Chem.*, 2008, **80**, 4634.

23 R. H. Kimura, E. R. Steenblock and J. A. Camarero, *Anal. Biochem.*, 2007, **369**, 60.

24 Y. P. Kim, Y.-H. Oh, E. Oh and H.-S. Kim, *Biochip J.*, 2007, **1**, 228.

25 P. C. Ray, A. Fortner and G. K. Darbha, *J. Phys. Chem. B*, 2006, **110**, 20745.

26 C. A. Mirkin, R. L. Letsinger, R. C. Mucic and J. J. Storhoff, *Nature*, 1996, **382**, 607.

27 Y.-P. Ho, H. H. Chen, K. W. Leong and T.-H. Wang, *J. Controlled Release*, 2006, **116**, 83.

28 J. Lee, Y. Choi, J. Kim, E. Park and R. Song, *Chemphyschem*, 2009, **10**, 806.

29 A. Krishnan, T. S. Sreeremya, E. Murray and S. Ghosh, *J. Colloid Interf. Sci.*, 2013, **389**, 16.

30 T. S. Sreeremya, A. Krishnan, L. N. Satapathy and S. Ghosh, *RSC Adv.*, 2014, **4**, 28020.

31 F. Dang, K. Kato, H. Imai, S. Wada, H. Haneda and M. Kuwabara, *Cryst. Growth Des.*, 2010, **10**, 4537.

32 M. G. Bellino, D. G. Lamas and N. E. W. de Reca, *Adv. Funct. Mater.*, 2006, **16**, 107.

33 S. Ramesh, K. C. J. Raju and C. V. Reddy, *Trans. Ind. Ceram. Soc.*, 2013, **70**, 143.

34 T. S. Sreeremya, A. Krishnan, A. P. Mohamed, U. S. Hareesh and S. Ghosh, *Chem. Eng. J.*, 2014, **255**, 282.

View Article Online
DOI: 10.1039/C4RA17326K

35 I. Hrianca, C. Caizer and Z. Schlett, *J. Appl. Phys.*, 2002, **92**, 2125.
36 T. S. Sreeremya, K. M. Thulasi, A. Krishnan and S. Ghosh, *Ind. Eng. Chem. Res.*, 2012, **51**, 318.
37 M. Amjadi and L. Farzampour, *Luminescence*, 2013, **29**, 689.
38 X. G. Zhang, J. L. Zhang, Z. Y. Dong, J. X. Shi and M. L. Gong, *J. Lumin.*, 2012, **132**, 914.
39 U. Anand, C. Jash, R. K. Boddepalli, A. Shrivastava and S. Mukherjee, *J. Phys. Chem. B*, 2011, **115**, 6312.
40 R. Koole, P. Liljeroth, C. D. Donega, D. Vanmaekelbergh and A. Meijerink, *J. Am. Chem. Soc.*, 2007, **129**, 10613.
41 S. Xu, S. Xu, Y. Zhu, W. Xu, P. Zhou, C. Zhou, B. Dong and H. Song, *Nanoscale*, 2014, **6**, 12573.
42 J. Zhang, B. Li, L. Zhang and H. Jiang, *Chem. Commun.*, 2012, **48**, 4860.
43 A. Ahniyaz, Y. Sakamoto and L. Bergstrom, *Cryst. Growth Des.*, 2008, **8**, 1798.
44 N. Du, H. Zhang, B. Chen, X. Ma and D. Yang, *J. Phys. Chem. C*, 2007, **111**, 12677.
45 Y. Li and W. Shen, *Chem. Soc. Rev.*, 2014, **43**, 1543.
46 D. L. Monika, H. Nagabhushana, R. H. Krishna, B. M. Nagabhushana, S. C. Sharma and T. Thomas, *RSC Adv.*, 2014, **4**, 38655.
47 G. A. Kumar and N. V. Unnikrishnan, *J. Photochem. Photobiol., A*, 2001, **144**, 107.
48 E. Gokoglu and E. Yilmaz, *J Fluoresc.*, 2014, **24**, 1439.
49 J. R. Kanicky and D. O. Shah, *J. Colloid Interf. Sci.*, 2002, **256**, 201.
50 I. M. El-Anwar and S. A. El-Henawii, *J. Mater. Sci. Technol.*, 1998, **14**, 361.
51 R. Tadmor, R. E. Rosensweig, J. Frey and J. Klein, *Langmuir*, 2000, **16**, 9117.